12-2018

Inter-Laminar Fracture of 3D-Printed Plastics - Development of Methods

Christopher Stolinski
Utah State University

INTER-LAMINAR FRACTURE OF 3D-PRINTED PLASTICS - DEVELOPMENT OF METHODS

by

Christopher Stolinski

A report submitted in partial fulfillment
of the requirements for the degree

of

MASTER OF SCIENCE

in

Mechanical and Aerospace Engineering

Approved:

_____	_____
Dr. Ryan Berke, Ph.D.	Dr. Thomas Fronk, Ph.D.
Major Professor	Committee Member

_____
Dr. Ling Liu, Ph.D.
Committee Member

UTAH STATE UNIVERSITY
Logan, Utah

2018

ABSTRACT

Inter-laminar fracture of 3D-printed plastics – Development of Methods

by

Christopher Stolinski, Master of Science

Utah State University, 2018

Major Professor: Dr. Ryan Berke
Department: Mechanical and Aerospace Engineering

A Split Hopkinson Pressure Bar (SHPB) is used to impart dynamic loads on a novel four-point bending specimen. The specimens are made of 3D printed acrylonitrile butadiene styrene (ABS) plastic and are subject to mode I fracture by the SHPB. The specimens are loaded in one orientation at one loading rate, and are recorded throughout deformation by a high-speed camera. The images are post-processed with a commercial Digital Image Correlation (DIC) software package to compute full-field displacements of pixel subsets, and are used to compute Crack Opening Displacement (COD) of the specimen. COD along with load are used to determine the failure energy of the specimens. This project is a development of methods and improvement of test equipment to enable further use of these techniques by Dr. Ryan Berke's lab at Utah State University. The methods presented, and work currently being performed by other students, will be used for future research in this lab.

(23 pages)

PUBLIC ABSTRACT

Inter-laminar fracture of 3D-printed plastics – Development of Methods

Christopher Stolinski

Due to the increased use of 3D printed acrylonitrile butadiene styrene (ABS) plastic parts, a way to quantify the failure energy (energy needed to initiate cracking) is needed. Impact tests at high rates of loading are performed to determine failure energy. Throughout testing, specimens are monitored with high speed cameras to perform camera-based deformation measurements. Data acquisition and processing methods to calculate failure energy using crack opening displacement, and loading rates are developed to enable further use by Dr. Ryan Berke's lab at Utah State University.

ACKNOWLEDGMENTS

I would like to thank Dr. Ryan Berke for proposing this research project, and working with me throughout the research process. A special thanks to Dr. Owen Kingstedt, assistant professor at the University of Utah, for allowing us to use his high-speed camera for data collection, and sharing his knowledge of the Split Hopkinson Pressure Bar with our lab group. I would also like to thank my committee members for taking time to review and provide feedback on my research.

I want to give a special thanks to my family, and friends for providing me with endless encouragement, support, and patience as I progressed through this project.

Christopher Stolinski

CONTENTS

Page

ABSTRACT iii
PUBLIC ABSTRACT iv
ACKNOWLEDGMENTS v
LIST OF TABLES vii
LIST OF FIGURES viii
LIST OF SYMBOLS ix
INTRODUCTION 1
OBJECTIVES 3
METHOD 4
Split Hopkinson Pressure Bar 4
Butterfly Specimen 6
Specimen Orientation 6
Loading Rates 7
Digital Image Correlation 9
Crack Opening Displacement 10
Failure Energy 10
RESULTS 11
Loading on Specimen 11
Crack Opening Displacement 12
Failure Energy 13
DISCUSSION 16
Split Hopkinson Pressure Bar 16
Butterfly Specimen 17
Specimen Orientation 18
Digital Image Correlation 18
Failure Energy 19
CONCLUSION 20
REFERENCES 21
APPENDICES 22

LIST OF TABLES

Table Page

Table 1. ABS plastic properties 22
Table 2. SHPB properties 22
Table 3. Manufacturer 3D Printer specifications 23

LIST OF FIGURES

Figure Page

Figure 1. Diagram of Split Hopkinson Pressure Bar system 4
Figure 2. Strain vs time from an ABS “butterfly” specimen test..... 5
Figure 3. "Butterfly” specimen geometry 6
Figure 4. Print orientations 7
Figure 5. Determine the beginning and ending of the strain wave pulses and overlapping strain wave plots 8
Figure 6. Plot of force vs time on specimen ends 8
Figure 7. Speckle pattern with DIC digital extensometer points and pre-crack tip marker 9
Figure 8. Loading on the specimen by the incident and transmission bars 11
Figure 9. Plot of the smoothed and unsmoothed loading curves vs time 12
Figure 10. Plot of COD using 3 different y values above the pre-crack tip 13
Figure 11. Plot of the smoothed and unsmoothed COD curves vs time 13
Figure 12. Plot of Force and COD vs time with critical points marked 14
Figure 13. Diagram of the loading due to the bending moment 15
Figure 14. Plot of strain vs time showing errant strain gauge signals 16
Figure 15. Updated butterfly specimen with dimensions 17
Figure 16. Comparison of images using different lenses on the high-speed camera..... 18
Figure 17. SHPB test equipment in lab..... 22

LIST OF SYMBOLS

A_b	area of bar
C	bar wave speed
d_{bar}	displacement of bar
E	modulus of elasticity
E_b	bar modulus of elasticity
ϵ_I	strain, incident wave
ϵ_T	strain, transmitted wave
ϵ_R	strain, reflected wave
F	force
FE	failure energy
I	area moment of inertia
KE	kinetic energy
L	length of striker bar
m	mass
μ	micro
M	moment
N	newton
P(x)	force as a function of displacement
P_I	force from incident bar
P_{II}	force from transmission bar
ρ	density
T	strain wave loading time
t_0	initial time
$t_{critical}$	time at fracture
U	strain energy
v	velocity

INTRODUCTION

Additive manufacturing (AM), also known as 3D Printing (3DP), has been gaining popularity over the past two decades. Though AM has been around for quite some time, the development of better technologies has allowed a broader use of AM parts. In 1968 Swainson developed a process to selectively fabricate a plastic pattern using three dimensional polymerization [1]. Later, AM was mainly used for rapid prototyping and casting inserts, and is more recently used to produce limited run structural parts and production tooling [1]. The expanded use of AM parts as structural components has increased the need for characterization of 3D printed materials, and over the past two decades there has been an increase in research published on AM material characterization. The expansive use of AM structural components in dynamic applications requires characterization of how these parts fail under high rates of loading, and how the laminar structure of the parts effects the failure energy. Currently, there is a lack of research in fracture of 3DP parts at high rates of loading.

When loading a 3DP part, the print orientation affects the strength of the part. The inherent anisotropy of printed parts, and the orientation of the laminar structure with respect to the direction of loading both play a part in the strength of the material. Ashtankar et al. [2] uses fused deposition modeling (FDM) to print specimens at varying angles from 0° to 90° while keeping all other parameters constant to show how tension and compression strength change due to print orientation only. Torrado and Roberson [3] use material extrusion 3D printing (ME3DP) for specimens of varying parameters to find a correlation between print raster pattern, specimen geometry, and print orientation to changes in ultimate tensile strength of acrylonitrile butadiene styrene (ABS). They show

how in tensile tests the ABS specimens have varying ultimate tensile strength depending on print orientation [3].

Recently a new four-point bending specimen – known informally as a "butterfly" specimen – was developed by Syn and Chen [4] to determine the effects of high-rate fracture on interfaces. The new specimen was designed to reduce error associated with misalignment with typical three-point bending specimens [4]. The specimen is loaded using a split Hopkinson pressure bar (SHPB), but requires custom aluminum supports to hold the specimen in place, and conductive paint to measure crack propagation during testing. Weerasooriya et al. [5] used the same specimen design to present the strength and failure energy for aluminum adhesive interfaces as a function of loading rate. Later, Whittie et al. [6] modified this specimen to work without the aluminum supports, thus allowing the specimen to be placed directly between the transmission and incident bars in a SHPB. Whittie's modified specimen was then used to measure the fracture response of cross-linked epoxy resins as a function of loading rate [6]. The crack propagation of the modified specimen was also measured differently. Digital Image Correlation (DIC) was used to determine the critical fracture point, and crack propagation velocity. To date, the specimen has yet to be used to study 3D printed materials.

The research presented here is a development of methods to use the "butterfly" specimen, presented by Whittie et al., to study high-rate interlaminar fracture in 3D printed plastics. Mode I fracture is achieved at high loading rates using a SHPB. The dependence of loading rate can be determined by failure energy and crack opening displacement (COD). The methods to determine loading rate and COD are presented with a discussion on best practices and a path forward for use of these methods in this lab.

OBJECTIVES

The objective of this project is to work toward quantifying the difference in failure energy of 3D-printed plastics depending on print orientation using a novel 4-point bending specimen under high load-rates using a Split Hopkinson Pressure Bar. This project is used to develop this testing method in Dr. Ryan Berke's lab at Utah State University. The methods presented, and work currently being performed by other students, will be used for future research in this lab.

- Reproduce portions of the experimental procedures detailed in Whittie et al.
- Characterize the anisotropic failure response of 3DP ABS plastic at high loading rates (on the order of $10^2\ to\ 10^4 s^{-1}$ [7]).
- Use methods developed for data acquisition and data processing to determine failure energy of the ABS plastic "butterfly" specimen.
- Develop a list of "best practices" to enable further use of these techniques by Dr. Berke's lab.

METHOD

Split Hopkinson Pressure Bar

The Split Hopkinson Pressure Bar (SHPB) is a system to impart dynamic loads on a specimen. The SHPB is able to produce strain rates from $10^2 s^{-1} to\ 10^4 s^{-1}$ [7]. The general set up of the SHPB system is shown in Figure 1.

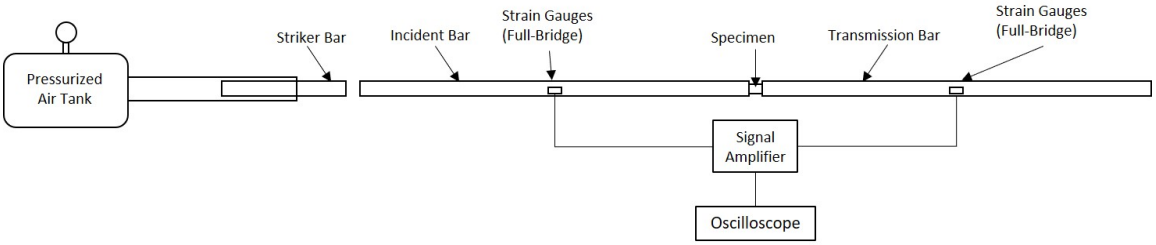

Figure 1. Diagram of Split Hopkinson Pressure Bar system

A specimen is placed between the incident and transmission bars. A pressurized air tank is used to launch the striker bar at the end of the incident bar. A stress wave from the impact moves through the incident bar at a fixed speed until it encounters the specimen. The theoretical speed of the wave, *C*, is a material property of the bar that is equal to Equation 1, where *E* is the elastic modulus of the bar and ρ is its density.

The theoretical bar wave speed is,

$$C = \sqrt{E_b/\rho}. \quad \text{Eq. 1}$$

The pulse width of the wave has a duration equal to the amount of time it takes for a wave to transmit to the opposite end of the striker bar and back. The pulse duration, *T*, can be computed by Equation 2, where *L* is the length of the striker bar.

$$T = \frac{2L}{C}. \qquad \text{Eq. 2}$$

Part of the stress wave is transferred through the specimen and continues on through the transmission bar, and part of the stress wave is reflected back through the incident bar. The stress waves are detected by strain gauges, one full-bridge on the incident bar, and one full-bridge on the transmission bar. The measured strain is quantified by voltage change on the strain gauges, and is amplified for data collection. The voltage along with time are recorded by an oscilloscope. The voltage from the strain gauges is converted to strain using the standard full-bridge strain gauge conversion equations. The strains are then used to compute high speed mechanical properties at the applied load rate. A plot of strain vs time calculated from the strain gauge voltage change is shown in Figure 2.

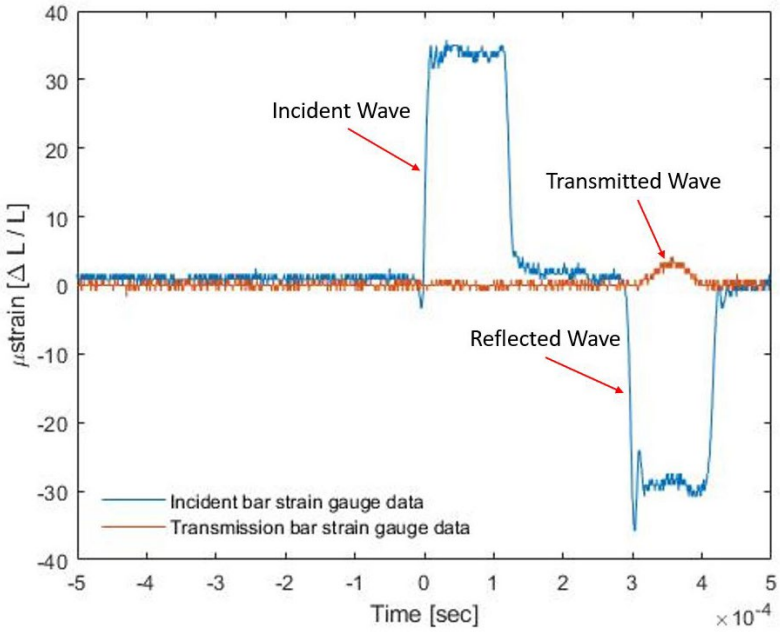

Figure 2. Strain vs time from an ABS “butterfly” specimen test

Butterfly Specimen

Figure 3 is a depiction of the modified butterfly, or four-point bend, specimen geometry developed by Whittie et al. [6], and the specimen that is used for this project. This specimen was developed to reduce the misalignment of three-point bend test specimens. The other benefit of this specimen is it doesn't need a special fixture to hold the specimen in the bars during testing.

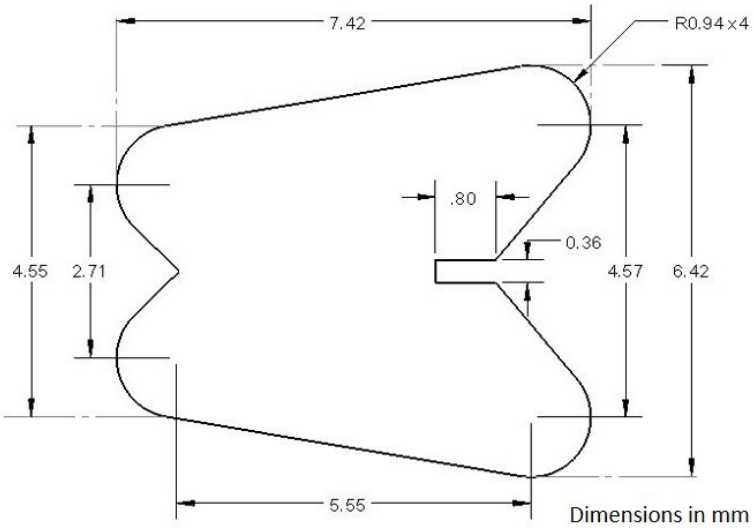

Figure 3. "Butterfly" specimen geometry

Specimen Orientation

The specimen will be loaded in three orientations denoted as 1, 2, and 3 in Figure 4 below. Print orientation number 3 is expected to have the lowest failure energy as the crack will propagate between print layers causing inter-laminar fracture. Print orientation number 2 is expected to have the highest failure energy since the crack will have to propagate normal to the print layers. Print orientation number 1 is expected to have a failure energy that is somewhere between orientations 2 and 3.

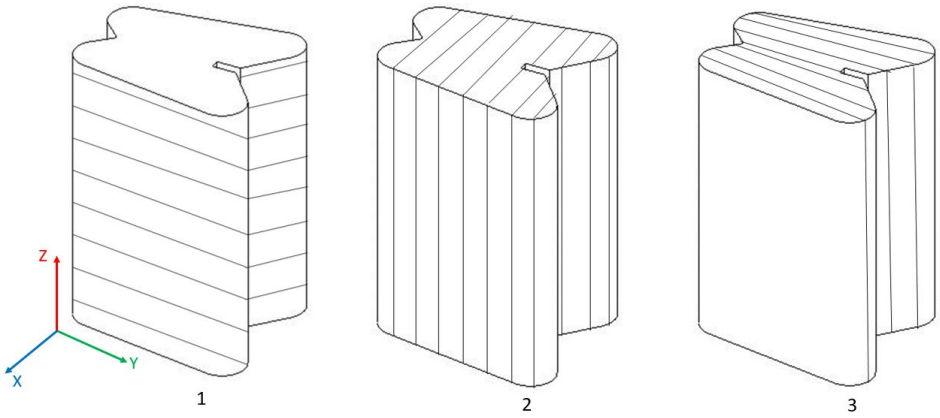

Figure 4. Print orientations

Loading Rates

The loading rates are determined by plotting the strain vs time data that is obtained from the strain gauges on the SHPB and depicted in Figure 2. The beginning and ending of the three strain waves, incident, reflected, and transmitted, are determined by picking the incident strain wave starting point and calculating the end of the incident wave and the beginning and ending of the reflected and transmitted waves as seen in Figure 5a). This is done by knowing the theoretical bar wave speed, C in Equation 1, and the loading time, T in Equation 2. The three waves are then plotted over one another, and adjusted by moving the bar wave speed, and starting point, up or down slightly to until they match as well as possible for a given data set. Figure 5b) shows what a good overlap of strain waves looks like. After the three strain waves are plotted together the force on the specimen ends is calculated using Equations 3 and 4, and plotted as seen in Figure 6. The equations for force on the specimen ends are denoted by P_I as the force from the incident bar, and P_{II} as the force from the transmission bar. The slope of the force plotted vs time will give the loading rate. The loading rates are correlated to a specific pressure that the striker bar is fired at.

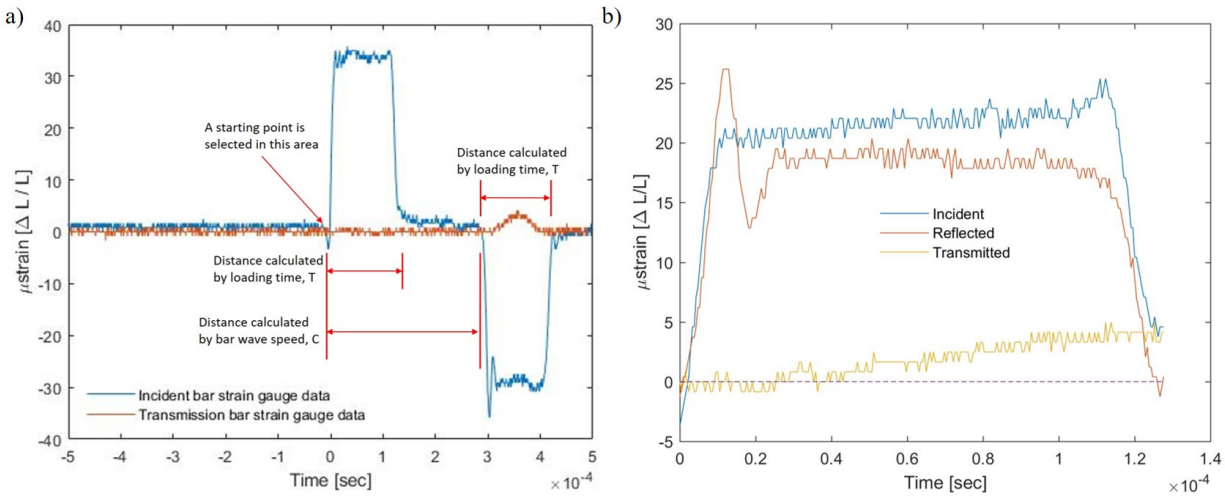

Figure 5. Determine the beginning and ending of the strain wave pulses and overlapping strain wave plots

$$P_I = E_b A_b (\epsilon_I + \epsilon_R) \quad \text{Eq. 3}$$

$$P_{II} = E_b A_b \epsilon_T \quad \text{Eq. 4}$$

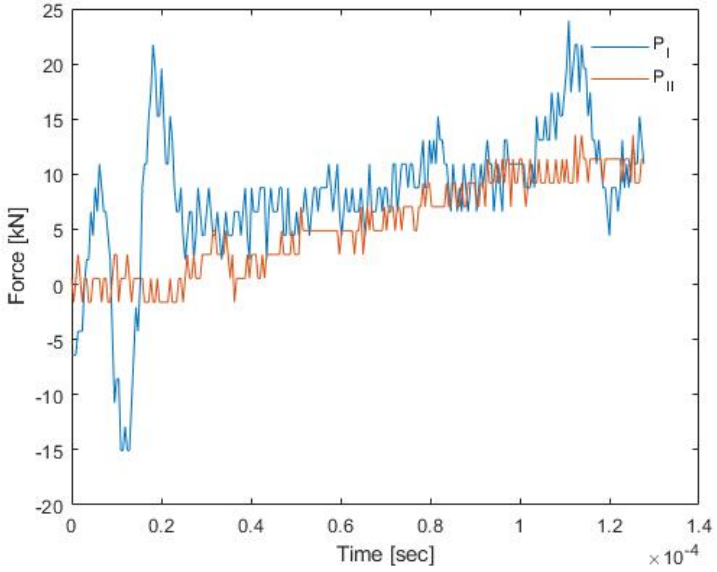

Figure 6. Plot of force vs time on specimen ends

Digital Image Correlation

The butterfly specimens are monitored throughout deformation by a high-speed camera. A Shimadzu HPV-X2 high-speed camera is used to capture the images that are used for DIC. The camera is set to take pictures at 666,667 frames per second (fps) with a resolution of 400 x 250, and exposure time of 1000ns. The working distance from the camera, not counting the lens, to the specimen is 10in. The lens used with the camera is a Tonika macro 100mm f2.8.

Images from the camera are used to compute displacements via Digital Image Correlation (DIC). Displacements are measured on the surface of a solid specimen by tracking deformation through a set of images. The specimen is painted with a non-uniform speckle pattern as shown in Figure 7. The images of a dynamic event are processed through a commercial DIC software package, VIC-2D, that measures the full-field displacement of pixel subsets, which can then be used to compute full-field strains. The subset and step-size used for the correlation in VIC-2D is 31 and 1, respectively.

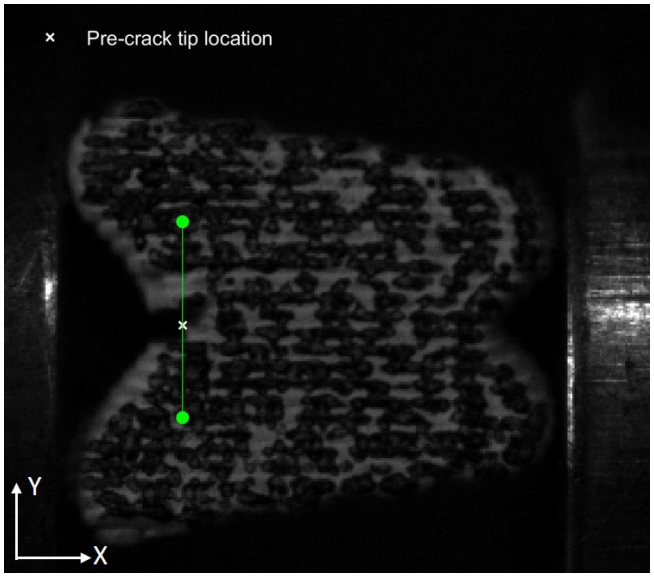

Figure 7. Speckle pattern with DIC digital extensometer points and pre-crack tip marker

Crack Opening Displacement

The reported displacement data from VIC-2D is used to create a digital extensometer to measure the COD. The movement of points above and below the crack plane, as seen in Figure 7, are tracked through sequential images of an impact test. The relative displacement of these points is used to plot COD vs time. COD is used along with load to determine the point of fracture initiation in the specimen.

Failure Energy

The load applied to the specimen and COD is plotted vs time. Equation 5 is used to determine the failure energy of the specimen [6], where *P(x)* is the load as a function of displacement, and $t_0 \rightarrow t_{critical}$ is the time from initial impact to time of crack initiation. The failure energy is calculated for one orientation and one loading rate to develop the methods presented. Then failure energy will be compared between all three orientations, and between loading rates after future tests are conducted.

$$FE = \int_{t_0}^{t_{critical}} P(x)dx \quad \text{Eq. 5}$$

RESULTS

Loading on Specimen

The specimens are loaded at 5psi, which is equivalent to a loading rate of $125.7\ N/\mu sec$. A diagram of the loading, denoted as $P_I\ and\ P_{II}$, on the specimen is shown in Figure 8. Loading is plotted vs time in Figure 6 up to the maximum load. Since there is a force equilibrium on both ends of the specimen the force calculated from the incident bar or the transmission bar can be used in the failure energy calculations. The load from the transmission bar, P_{II}, is used to calculate failure energy for this report. The loading signal from the transmission bar is smoothed to reduce the noise associated with the signal. The original and smoothed force curves are plotted together in Figure 9 to show there is no significant loss of data due to smoothing.

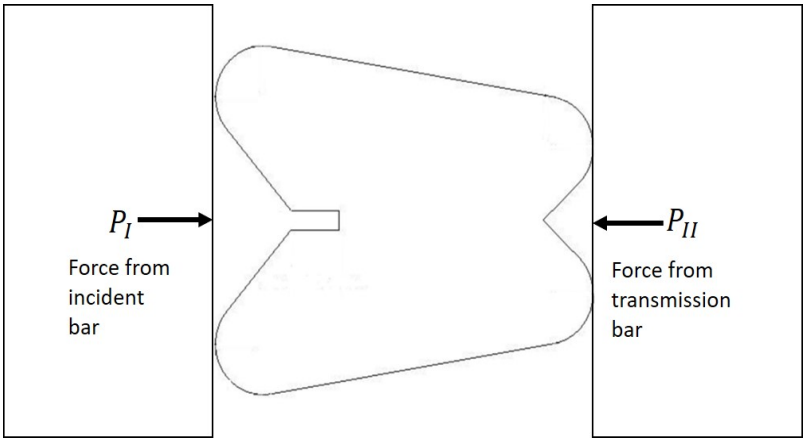

Figure 8. Loading on the specimen by the incident and transmission bars

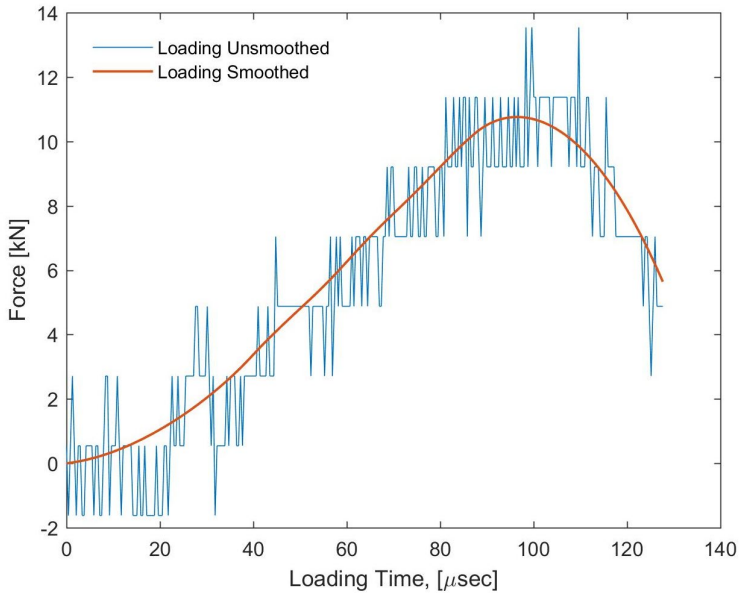

Figure 9. Plot of the smoothed and unsmoothed loading curves vs time

Crack Opening Displacement

Using data from processing high-speed camera images in the VIC-2D software COD at the pre-crack tip is calculated. Figure 7 is the specimen marked with the location of the pre-crack, and the points used to calculate COD. The point in the x-direction is fixed based on the location of the pre-crack tip. The points in the y direction are chosen arbitrarily as long as they are on opposite sides of the cracking plane, and data output from the displacement correlation in VIC-2D results in enough data from initial loading to specimen fracture to calculate COD. To show that the y value is arbitrary 3 different values of y in line with the the pre-crack tip are used to plot COD and are shown in Figure 10. The figure shows the assumption that y is arbitrary holds since all three curves lie on top of one another. Figure 11 is a plot of the smoothed vs unsmoothed COD curve to show that smoothing the COD curve doesn't result in a significant loss of data. The point determined to be the critical COD is marked.

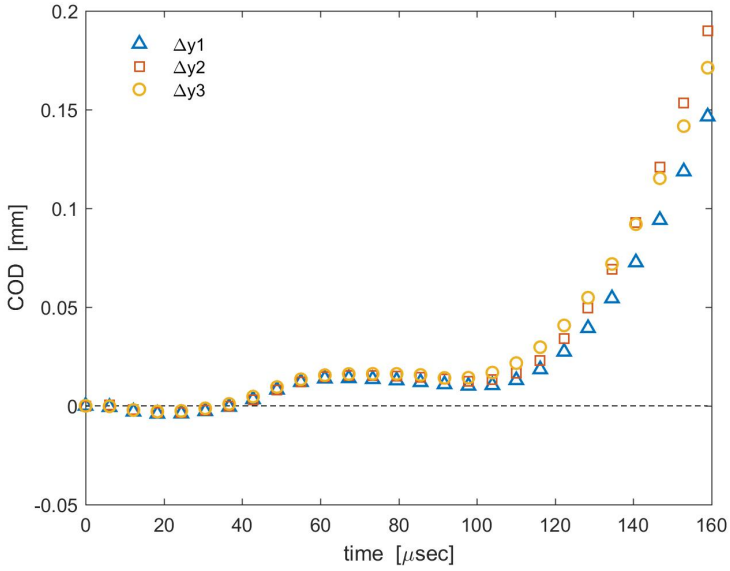

Figure 10. Plot of COD using 3 different y values above the pre-crack tip

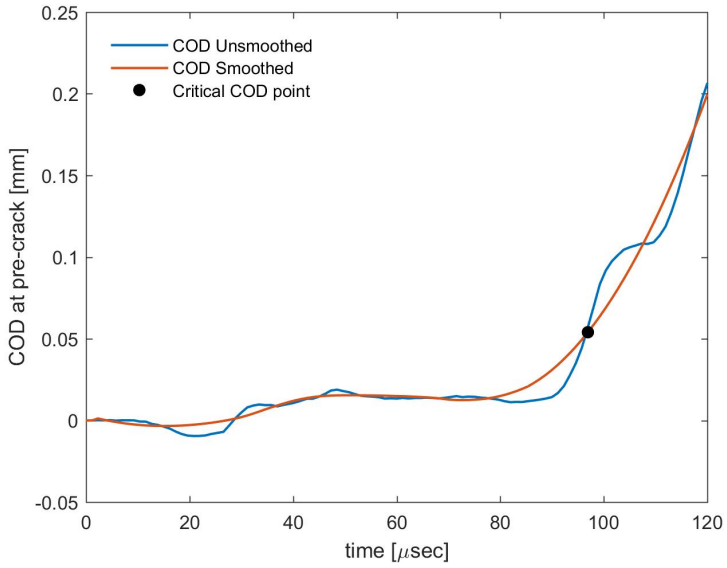

Figure 11. Plot of the smoothed and unsmoothed COD curves vs time

Failure Energy

The failure energy results are for a specimen in the X direction, which is orientation 3 in Figure 4, at a loading rate of 125.7 $N/\mu sec$. COD is calculated by tracking the two points in Figure 7 which coincide with the pre-crack tip, from initial

loading to specimen fracture. Figure 12 is a plot of force and COD vs time with data markers on the COD curve showing the discrete images used to calculate COD. The plot shows where max load and fracture on the loading and COD curves occur, respectively.

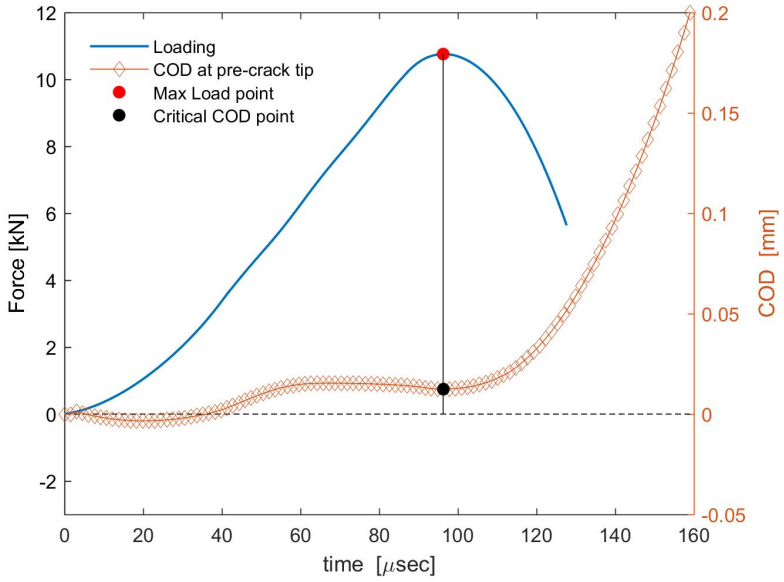

Figure 12. Plot of Force and COD vs time with critical points marked

Failure energy is calculated by Equation 6,

$$FE = F * d_{bar} \ . \qquad \text{Eq. 6}$$

The force applied in the x-direction multiplied by the total displacement from $t_0 \rightarrow t_{critical}$ results in the total energy of the system required to initiate fracture in the specimen. To obtain the failure energy an approximation of the kinetic energy (KE) and strain energy (U) are determined by Equations 7, and 8.

$$KE = \frac{1}{2}mv^2, \qquad \text{Eq. 7}$$

$$U = \frac{1}{2E}\int \frac{M(y)^2}{I(y)}dy \ . \qquad \text{Eq. 8}$$

Where m is the mass of the incident bar, v is the velocity of the bar from $t_0 \rightarrow t_{critical}$ in Equation 7. In Equation 8, M is the internal bending moment on the crack tip which varies as a function of y, E is the modulus of elasticity, and I is the area moment of inertia which varies as a function of y. Since the KE and U are much smaller than the total failure energy, $2.4\ kJ\ and\ 703\ J$ respectively, they can possibly be neglected. The resulting failure energy for the specimen is $199\ kJ$.

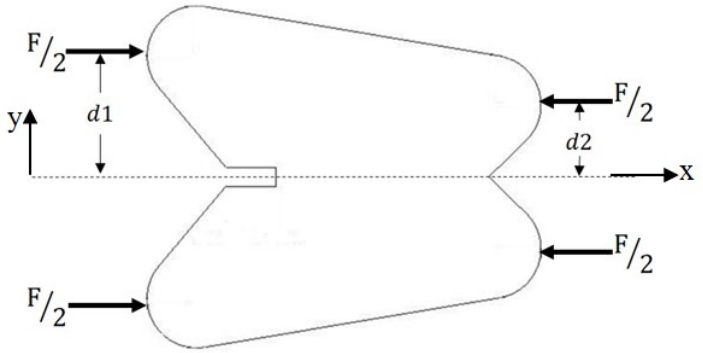

Figure 13. Diagram of the loading due to the bending moment

The U is only an approximation since the specimen is assumed to be a simple beam to calculate M and I, and the modulus of elasticity is estimated. There is a wide range of values for the modulus of elasticity for 3DP ABS so an average is used. Due to the approximations further research is needed to verify the result. One way to verify the result is to apply the methods of integrating under the load vs COD curve presented for the remaining two orientations to determine if those results agree with the expected results, but more research is required to use this method.

DISCUSSION

The methods presented are shown to be sufficient to gather all relative data from the SHPB to calculate forces on the specimen. The impact event is captured by a high-speed camera with enough images and resolution to successfully correlate all displacements in the VIC-2D commercial software. The code written to process the bar and camera data works as expected. However, there are improvements that need to be made on the test equipment, and the calculation of the failure energy. These tasks will be accomplished by a future grad student already selected by Dr. Berke. The deficiencies that will be addressed are discussed below with possible corrections for each deficiency.

Split Hopkinson Pressure Bar

During testing a malfunction on the test set occurred due to a broken wire on the strain gauge bridge junction on the incident bar. Due to the extensive work needed to remove and reapply the wiring to the strain gauge bridge junction testing was delayed until the bar was fixed. The data shows there is an errant signal in incident bar during testing shown in Figure 14.

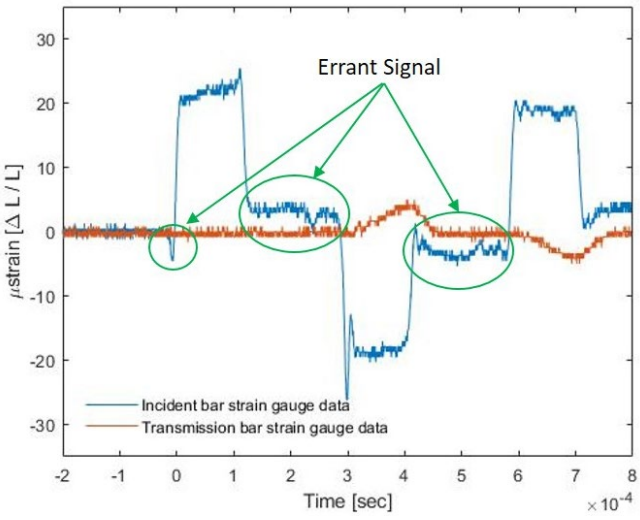

Figure 14. Plot of strain vs time showing errant strain gauge signals

The signal starts at zero as it should, but the signal has a momentary negative drop in strain that occurs before the expected large positive strain is recorded by the oscilloscope. The strain should return to zero after the strain wave passes, but the strain gauge holds a voltage and never returns to zero. After the repairing the strain gauge bridge junction the errant signal remained. This is evidence of a bigger problem in the incident bar that will need to be fixed in order for testing to resume. The electrical system used to record the data will be checked first. If there are no electrical issues causing the problem the next step would be to remove and reapply new strain gauges to the bar.

Butterfly Specimen

The original butterfly specimen was printed with a pre-crack. It was realized later that by printing the pre-crack the normal stress concentrations due to the crack would not be present. Figure 15 shows the updated butterfly specimen without a pre-crack. The updated specimens will have a pre-crack cut into them using a high-speed slitting saw that is 0.5 mm thick.

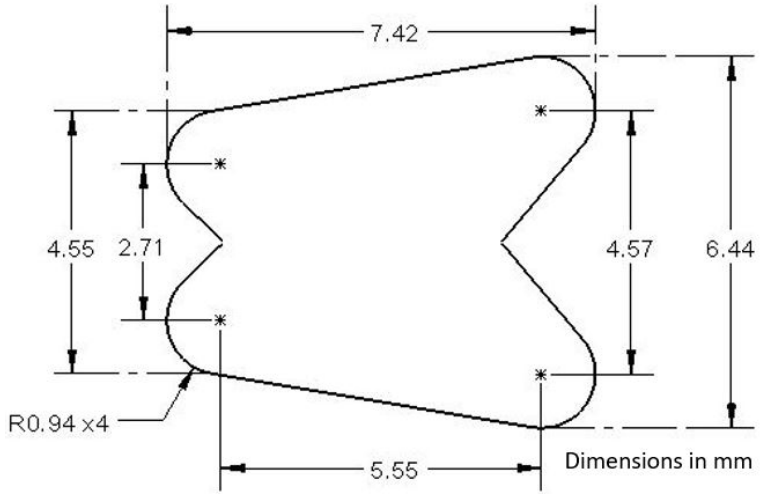

Figure 15. Updated butterfly specimen with dimensions

Specimen Orientation

Due to the issues with the SHPB only one of the three proposed orientations, the X orientation in Figure 4, was tested.

Digital Image Correlation

The first round of test results with the high-speed camera using a Nikon 50mm lens resulted in images of the specimen that were too small to correlate with the commercial DIC software. Figure 16a) shows the specimen using the 50mm lens which takes up 33 x 29 of the full 400 x 250 resolution of the camera. A new lens was then made available to the lab. A 100mm macro lens is used in subsequent tests to fill the image with the specimen as seen in Figure 16b) which increased the resolution of the specimen to 210 x 191 of the full 400 x 250 resolution of the camera.

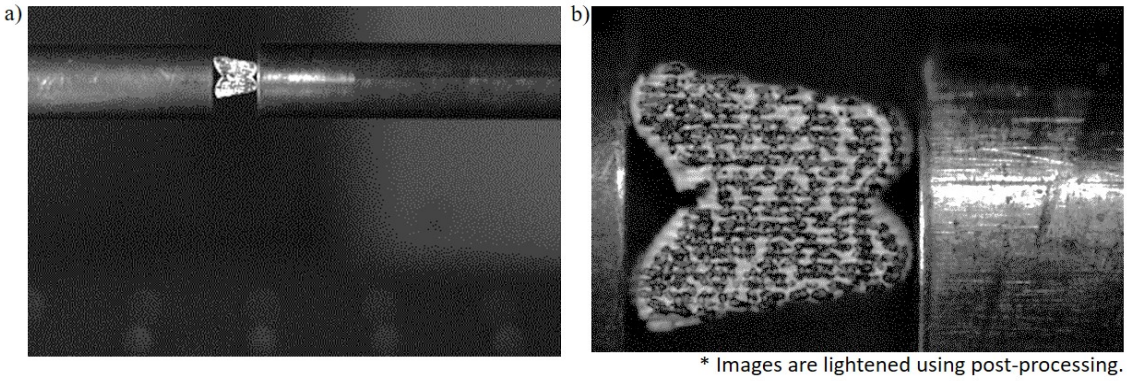

Figure 16. Comparison of images using different lenses on the high-speed camera

Failure Energy

The method of determining failure energy of the specimen as the area under the loading curve from $t = 0$ to $t = critical\ COD$ of the specimen according to Equation 5 is determined to not be accurate. The force acting on the specimen is in the x-direction and the COD is in the y-direction, therefore failure energy cannot be determined by integrating the load vs COD curve directly. The Whittie et al. paper [6] where Equation 5 comes from has some restrictions that aren't clearly explained. This method will not be abandoned as this method can be easier to use compared to the method used for the results presented in this report, but more research is required to use this method.

CONCLUSION

The methods presented are developed to enable further use of these techniques by Dr. Berke's lab at Utah State University. Dynamic loading on 3D printed plastics using a novel "butterfly" specimen in a Split Hopkinson Pressure Bar is described along with results for one specimen orientation at one loading rate. Total energy absorbed by the specimen to initiate fracture is calculated. The failure energy calculated for 3D printed ABS plastic in this orientation and loading rate is 199 kJ. Discussion on the effects of anisotropy due to print orientation cannot be presented at this time since only one orientation was successfully completed. The methods presented will be used in the lab to obtain failure energy for the remaining 2 orientations when the deficiencies with the bar are addressed. The equipment to image the impact at high-speed is known to work by the presented data. Data processing code is written and shown to work for the strain and image data that is recorded for the specimen impact. The use of these methods and data processing techniques will be used in Dr. Berke's lab to finish this research, and will be incorporated into other research projects moving forward.

REFERENCES

[1] D. L. Bourell and J. J. Beaman, “A Brief History of Additive Manufacturing and the 2009 Roadmap for Additive Manufacturing: Looking Back and Looking Ahead,” p. 7, 2009.

[2] K. M. Ashtankar, D. A. M. Kuthe, and B. S. Rathour, “RAPID PROTOTYPING STYRENE (ABS) PARTS,” p. 7, 2013.

[3] A. R. Torrado and D. A. Roberson, “Failure Analysis and Anisotropy Evaluation of 3D-Printed Tensile Test Specimens of Different Geometries and Print Raster Patterns,” *J. Fail. Anal. Prev.*, vol. 16, no. 1, pp. 154–164, Feb. 2016.

[4] Chul Jin Syn and W. W. Chen, “Surface Morphology Effects on High-Rate Fracture of an Aluminum/Epoxy Interface,” *J. Compos. Mater.*, vol. 42, no. 16, pp. 1639–1658, Aug. 2008.

[5] T. Weerasooriya, C. A. Gunnarsson, R. Jensen, and W. Chen, “Strength and Failure Energy for Adhesive Interfaces as a Function of Loading Rate,” in *Dynamic Behavior of Materials, Volume 1*, T. Proulx, Ed. New York, NY: Springer New York, 2011, pp. 67–76.

[6] S. Whittie, P. Moy, C. A. Gunnarsson, D. Knorr, T. Weerasooriya, and J. Lenhart, “Fracture Response of Cross-Linked Epoxy Resins as a Function of Loading Rate,” in *Dynamic Behavior of Materials, Volume 1*, V. Chalivendra, B. Song, and D. Casem, Eds. New York, NY: Springer New York, 2013, pp. 7–15.

[7] W. Chen and B. Song, *Split Hopkinson (Kolsky) Bar*. Boston, MA: Springer US, 2011.

APPENDICES

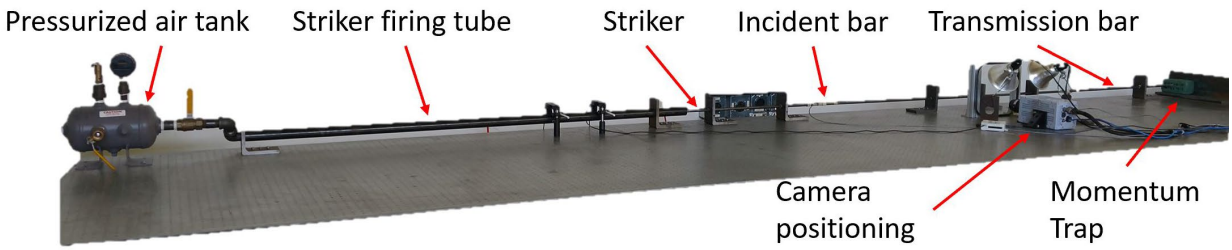

Figure 17. SHPB test equipment in lab

Table 1. ABS plastic properties

Mechanical Properties		**Physical Properties**	
Hardness, Rockwell R	103 - 112	Density, ρ [g/cc]	1.04
Tensile Strength, Yield [MPa]	42.5 - 44.8	Melt Flow [g/10 min]	18 - 23
Elongation Break [%]	23 - 25		
Flexural Modulus [GPa]	2.25 - 2.28		
Flexural Yield Strength	60.6 - 73.1		

Table 2. SHPB properties

Material	4140 steel	**Bars**	**Bar lengths [m]**
Modulus of Elasticity [GPa]	205	Incident	1.521
Poisson's ratio [η]	0.29	Transmission	1.594
Theoretical bar wave speed, C_b [m/s]	5110	Striker	.3016
		Diameter (all bars)	.0127

Table 3. Manufacturer 3D Printer specifications

Fortus 250MC	
System Specifications	
Build Envelope (XYZ)	254 X 254 X 305 mm
Material Delivery	One build material cartridge: 923 cc
Material Options	ABSplus
Layer Thickness	0.178 mm
Support Structure	Soluble
Color	Black
Achievable Accuracy	±.241mm* *Accuracy is geometry-dependent. Achievable accuracy specification derived from statistical data at 95%-dimensional yield.